An Investigation into the Effect of Ventilation, Bulbs and Flow Turbulence on Lifting T Foil Performance

Iain Duncan
University of Strathclyde, Scotland, iainduncan00@gmail.com.

Thomas Goodman
University of Strathclyde, Scotland.

Margot Cocard
University of Strathclyde, Scotland.

Sandy Day
University of Strathclyde, Scotland.

Saishuai Dai
University of Strathclyde, Scotland.

Abstract.

Flapped lifting T foils are a key part of modern high-performance craft due to their ability to reduce wetted surface area and hence drag at high speed. The performance of these foils is significantly affected when ventilated. Ventilation on a T-foil normally leads to a dramatic and uncontrolled loss of lift and overall vessel drag increment due to the hull coming into contact with the water surface. Limited research of ventilated T foils has been published due to challenges associated with reproducing ventilations in a relatively low-speed tow tank environment.

The current study looks into the performance of a Waszp rudder fitted with modifications. The position of the horizontal foil relative to the vertical strut was varied as was the flow turbulence around the vertical strut using a turbulence stimulating wire. Towing test of the modified Waszp rudder was carried out at the Kelvin Hydrodynamics Laboratory of University of Strathclyde. Results were compared against the original Waszp T-foil.

Experimental testing results shows how the foil can be modified to the T foil performance. It also shows changes in the characteristics in the ventilated cavity when the foil is operating in fully ventilated flow. A new method capable of stimulating foil ventilation repeatably was developed utilizing turbulence wire which can potentially enable more T-foil ventilation-related experimental studies in the future.

Keywords: T-foil, ventilation, hydrodynamic tank testing

NOMENCLATURE

Cl – Coefficient of Lift
Cd – Coefficient of Drag

1. INTRODUCTION

Hydrofoils can substantially reduce the drag of the craft they are fitted to due to the lift produced allowing the boat to change from buoyancy to lift supported. This results in the hull lifting clear of the water surface. Reducing the wetted surface area lowers the friction drag allowing the craft to reach higher speeds for the same drive force. Drive force is a constant for a given windspeed making resistance reduction a key concern for designers, this has driven the adoption of hydrofoils in high performance craft.

The International Moth class has been at the forefront of foil development in racing dinghies over the last 20 years. With the current system, utilising a lifting T foil for both the main foil and the rudder, appearing successfully at the Moth Worlds in the early 2000s (Day, et al., 2019). This early adoption of the technology was primarily driven by the class being a development class with rules incentivising sailors and designers to innovate to improve boat performance.

The Moth class has seen constant advancement in foil design and performance, resulting in the class becoming financially prohibitive for many sailors due to the use of high-tech materials such as carbon fibre. This led to the design of the Waszp which entered production in 2016. It aims to use lower cost materials to make foiling affordable and accessible. Foiling boats are becoming more popular with less experienced sailors excited by the possibility of racing the one design Waszp class.

The existing work undertaken has typically focused on experimental testing due to the challenges in creating accurate CFD simulations capable of predicting multiphase flow. Several studies have tested flapped lifting T foils in an attempt to improve the ability for designers to predict the performance of a boat through the use of velocity prediction programs (Day, et al., 2019) (Andresson, et al., 2018) (Beaver & Zseleczky, 2009).

Dinghies operate in a range of flow conditions with partially and fully ventilated flow a realistic possibility. Fully ventilated flow occurs through two key mechanisms: Tip Vortex and Free Surface Filament Ventilation (Binns & Barden, 2012). Both mechanisms were observed to occur in the testing undertaken. For ventilation to occur the following conditions must be met: flow separation must occur, the free surface seal must be broke broken, there must be a low pressure region and a path to the free surface must be present (Binns & Barden, 2012). These parameters are key to developing a mechanism capable of triggering ventilation.

Ventilation is known to significantly impair the performance of the foil reducing the lift coefficient substantially (Korulla & Sha, 2012) leading to a loss of vertical equilibrium for the vessel. As a result of this the vessel ceases to foil and transitions back from buoyancy to lift supported. Through peer testing sailors have explored simple adaptations such as manipulating flow turbulence to improve foil performance. There is little robust published research into these simple solutions and it is this area this work builds on.

In recent years bulbs have become more common on both moth foils and Americas Cup yachts. These have been utilized to modify the shape of the junction between the horizontal and strut as well as allowing the position of the horizontal to be varied. Due to the highly competitive nature of these classes little data is available publicly and as a result this work attempts to provide initial evidence behind the designs.

2. TANK TESTING

2.1 Foil and modifications

The foil tested was a lifting T foil commercially available and normally used as the rudder of a high-performance sailing boat, the Waszp. This foil was selected due to it being known to suffer ventilation issues as a result of the limitations imposed on its shape due to the use of low cost materials. Aluminum is used for the construction of the majority of the foil with the tips of the horizontal being plastic. This is in contrast to many moth foils which use carbon fibre. The cross section of the foil is shown below in Fig. 1. Key dimensions of the horizontal are shown below in Tab. 1.

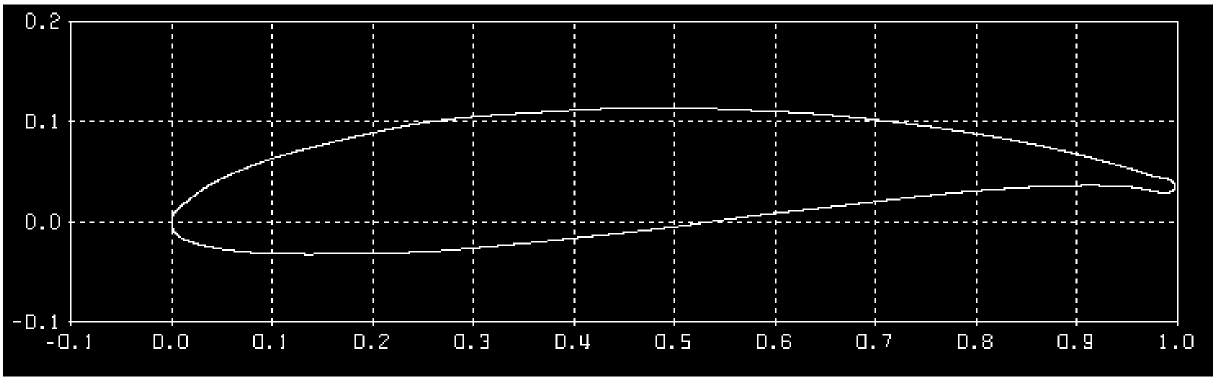

Figure 1. Horizontal foil cross section

Table 1. Key horizontal foil dimensions

Span	0.75m
Chord	0.14m
Planform Area	0.0958m
Thickness/Chord	13%
Camber/Chord	3.76%

Several modifications were made to the foil for testing: the addition of a bulb which allowed the horizontal to be moved relative to the leading edge of the strut; the addition of a second bulb at the junction between the strut and horizontal; and the fitting of a turbulence generating wire to various positions close to the leading edge of the strut. The bulb which moves the horizontal results in the leading edge being 150mm from the leading edge of the vertical. The wire was fitted to the strut and tested in four positions as shown below in Tab. 2. Nondimensional positions for the wire were calculated using the chord length of the horizontal. The modified and unmodified foil is shown below in Fig. 2.

Figure 2. Unmodified foil, foil with horizontal in aft position, foil with bulb, foil with horizontal in forward position

Table 2. Wire positions tested

Distance from leading edge of Horizontal	x/c from Horizontal chord length
10	0.07
20	0.14
30	0.21
40	0.28
50	0.35
60	0.43

2.2 Test rig

Kelvin Hydrodynamics Lab towing tank based at the University of Strathclyde was used for the testing. It has a length of 76m with a width of 4.6m. The rig, shown below in Fig. 3, was fitted with load cells capable of measuring force in the x and y directions.

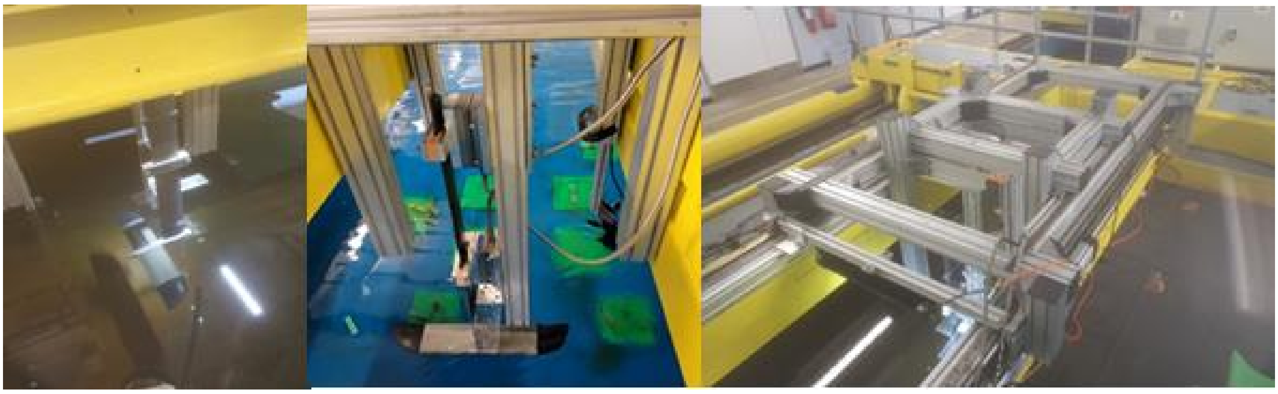

Figure 2. Testing rig

The load cells were calibrated using weights of known mass and a calibration factor applied. Spike computer software was utilised to allow average forces to be calculated. High speed and underwater cameras were used to determine the flow regime the foil was operating in. The characteristics of the ventilated cavity were observed using these images.

2.3 Testing conditions

The results presented in this paper are from two sets of tank testing conducted 12 months apart. The first set focussed on the ventilation with the second set focussed on quantifying the performance of the foil utilising lift drag coefficients.

Testing was conducted at speeds ranging from 0.475m/s to 4.092m/s corresponding to a Reynolds number range of $5.05*10^4$ and $4.35*10^5$. This is in comparison the Reynolds number seen when the Waszp is foiling with these likely to range from $9*10^5$ to $1.4*10^6$. These speeds are at the lower end of the likely speeds achieved by Waszp when it is foiling. The upper testing speed was limited by the design of the carriage. Hence ventilation had to be induced for the fully ventilated flow cases. A spray bottle capable of hitting the leading edge of the strut with a water jet was used to induce ventilation initially when required. The spray was aimed at the junction between the free surface and the strut. All testing was conducted at 0 yaw. The angle of the attack was 0 degrees for the non ventilated cases and -7.3 degrees for the ventilated cases. The depth of submergence was measured to the centre of the bulb fitted to move the horizontal with drafts marked and these utilised to test the other foil configurations.

Testing was conducted at 3 depths of submergence for the quantitative tests presented. These were 280mm, 140mm and 96mm. These corresponded to twice the horizontal chord, the horizontal chord and as close to half of the horizontal cord that was achievable with the experimental set up. Additional qualitative tests were conducted using different test conditions and images have been included in some areas.

3. FULLY WETTED FLOW
3.1 Effect of submergence on unmodified foil

Submergence has a significant impact on the lift with low submergence depths resulting in a reduction in lift as shown in Fig. 4 for the unmodified foil. Interaction between the free surface and the horizontal results in the flow being deflected upwards forming a wave behind the strut (Duncan, 1983) (Xing, et al., 2019). This leads to a change in the effective angle of attack and hence a reduction in the lift produced (Andersson & Granli, 2018). Visible differences in the flow behind the strut were observed with a larger aerated region forming at low submergence depths as shown in Fig. 5.

The drag coefficient was observed to be approximately equal at all depths of submergence at speeds greater than 1.5m/s, which is the area of interest due to typical sailing speeds. Measured drag was highest for the deepest submergence with this case also having the highest frontal area. Frontal area varied with depth of submergence and this is included in the calculation of the drag coefficients. A local maximum is apparent in the low speed range for 140mm submergence indicating a possible penalty for operating at specific speeds when the foil is near the free surface.

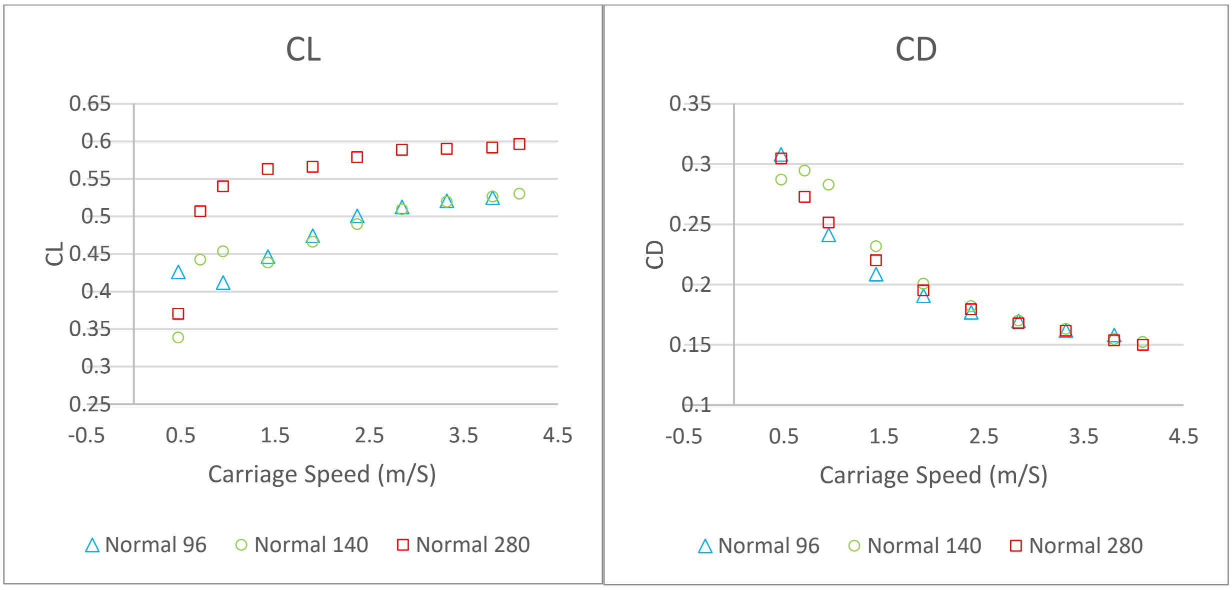

Figure 3. Lift and drag coefficients at varying depth of submergence for the unmodified foil

Figure 4. Free surface interaction of unmodified foil at 3.75m/s, 0 degrees – LH 88mm submergence RH 188mm submergence

3.2 Effect of submergence on modified foil

The lift coefficient was also observed to vary with the submergence for the modified foil with larger depths of submergence resulting in higher lift coefficients as shown below in Fig. 6 and Fig. 7. Below approximately 2m/s non linear effects are apparent with interactions with the free surface providing a potential explanation. Lift is increased at low depths of submergence and low speeds due to low pressure above the horizontal accelerating the flow as the free surface acts like a wall (Andersson & Granli, 2018).

The modified foil shows a reduced drag coefficient for larger depths of submergence. Significant peaks are apparent in the low speed region when the horizontal is moved aft when it is operating at 96mm and 140mm submergence. These peaks are much more pronounced with the horizontal in the aft position compared to the other two configurations tested.

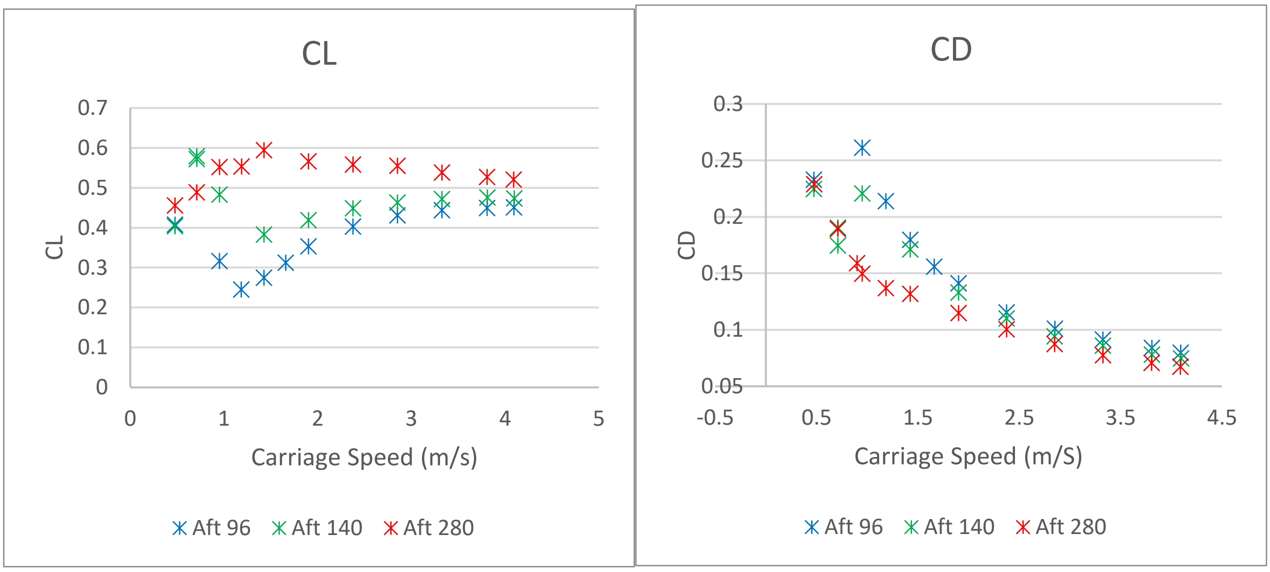

Figure 5. Lift and drag of foil with horizontal moved aft

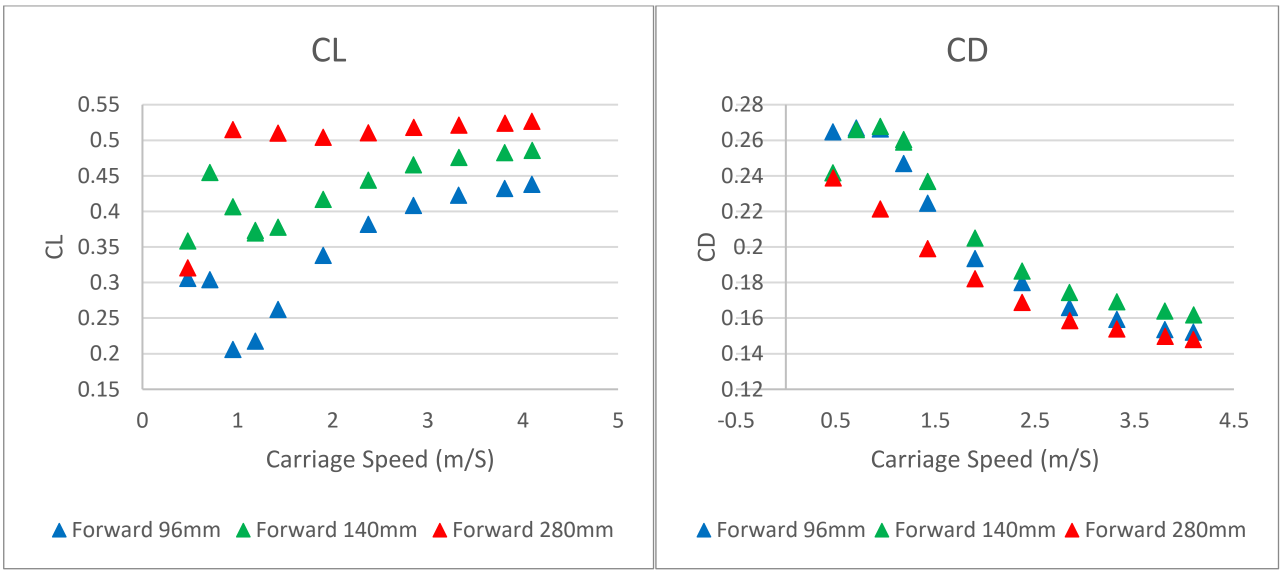

Figure 7. Lift and drag of foil with horizontal moved forward

3.3 Variation in lift drag ratio of foil due to depth of submergence

Shifting of the horizontal to the aft position results in a clear improvement in the lift drag ratio, as shown in Fig. 8 below, for the foil while it is operating at 140mm and 280mm submergence. A significant local maximum is visible again in the results at 140mm submergence below 2m/s. Operating at 96mm the optimum position of the horizontal is seen to vary with speed with both the aft and forward configurations showing a clear local minimum when the foil is operating at low speed. Though once again the aft position shows a clear benefit at higher test speeds. This demonstrates the importance of careful selection of depth of submergence and foil configuration if the foil is operating at low speeds.

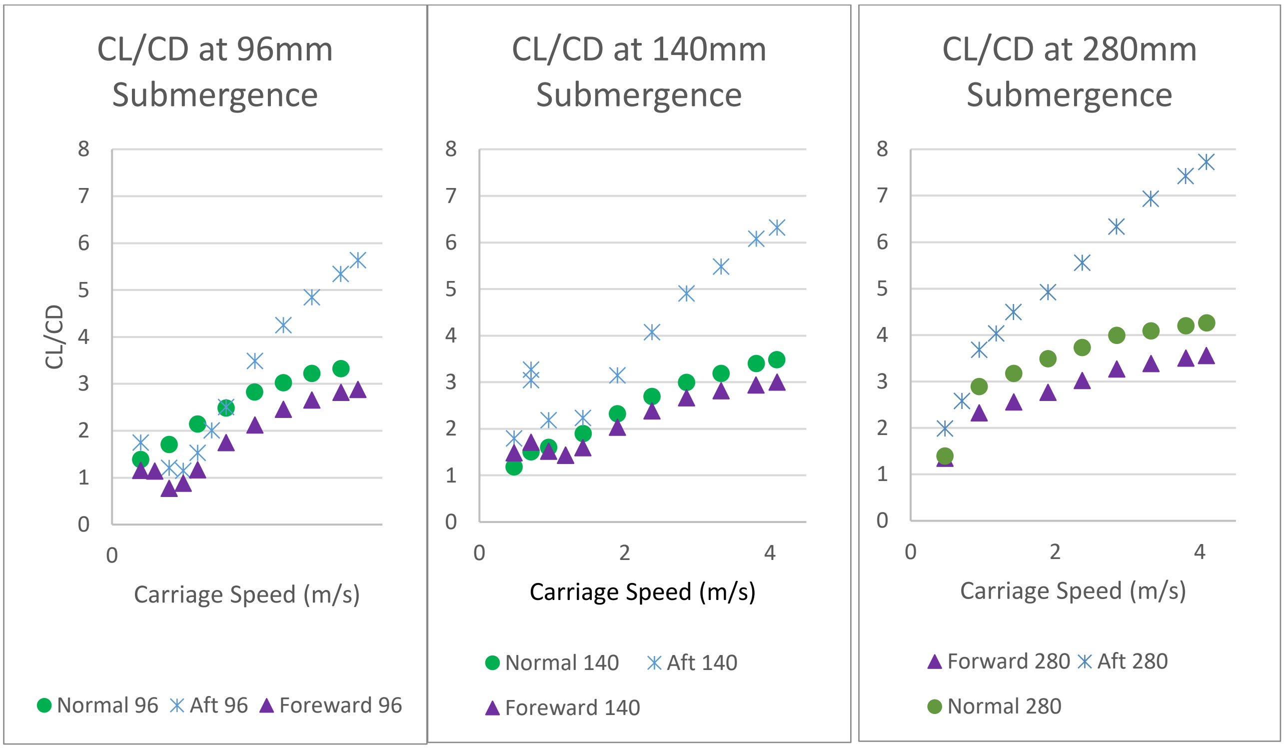

Figure 8. Lift Drag Coefficient Ratio at Different Submergences

It can be seen from Fig. 9 below that there is significantly greater variation in the drag coefficient than the lift coefficient, at 280mm submergence, when the position of the horizontal is changed.

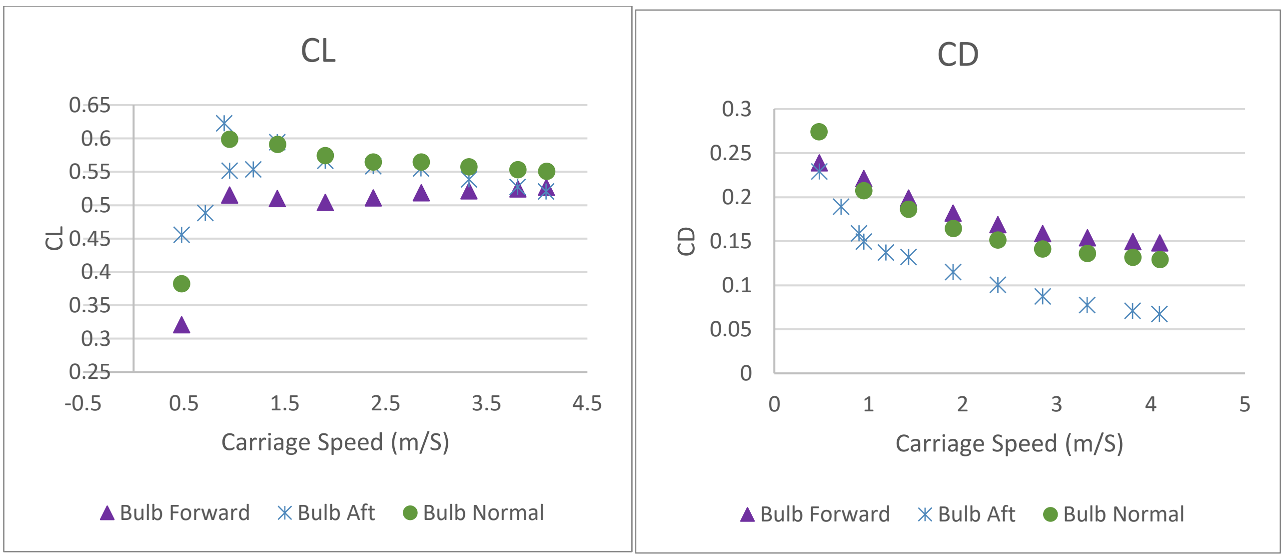

Figure 6. Lift and drag coefficients for 280mm submergence

Moving the horizontal backwards leads to a large drag reduction with a greater area of the horizontal operating in turbulent flow potentially accounting for this. At low speeds positioning the horizontal aft of the strut leads to the greatest lift coefficient. As speed increases the aft and forward lift coefficients converge with the forward position showing the higher lift coefficient at the greater speed tested.

3.4 Effect of flow turbulence and bulb on foil performance

The foil was fitted with a turbulence generating wire 10mm from the leading edge, this was selected as it was known to increase flow turbulence without resulting in the formation of a ventilated cavity. Testing was conducted with the wire fitted to the foil both with and without a 3D printed bulb which was attached to the junction between the strut and the horizontal. This bulb did not shift the position of the horizontal. All of the tests presented in this section are at 280mm submergence.

Fitting of the bulb at the junction between the horizontal and the vertical results in substantial reductions in the drag coefficient as shown in Fig. 10. The presence of the bulb in the junction will modify the horseshoe vortex that forms around the junction potentially accounting for the reduction in drag observed. Fitting of the turbulence generating wire results in an increase in the drag coefficient both with and without the bulb fitted. The wire results in the flow becoming turbulent earlier contributing to an increase in pressure drag as a result. Due to the low pressure region behind the strut increasing in size.

The effect of the modifications on the lift coefficient was observed to vary with the speed as shown in Fig. 10. Above 2m/s the unmodified foil has the largest lift coefficient though this is not the case when the foil is operating between 1m/s and 2m/s. Within this range we see fitting of the bulb and fitting of the bulb and wire together leads to an increase in the lift coefficient.

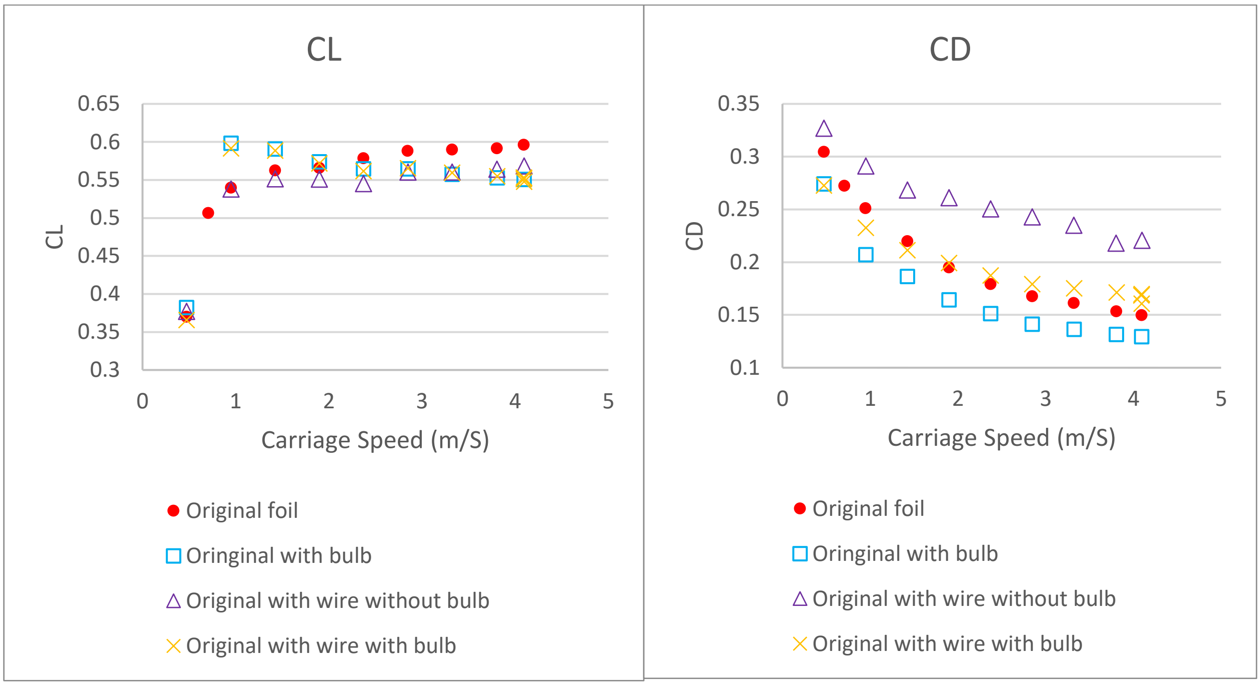

Figure 10. Lift and drag coefficients for the foil with increased turbulence and horizontal in normal position with bulb

Comparison of the lift drag ratio, shown below in Fig. 11, shows that the foil fitted with the bulb has the largest lift drag ratio at all speeds tested. The impact of fitting the turbulence generating wire along with the bulb is dependant on speed with the region between 1m/s and 2m/s being of interest once again. Reynolds numbers in this region range from $1.01*10^5$ to $2.13*10^5$. In this region only, does the addition of the wire along with the bulb show an improvement over the original foil.

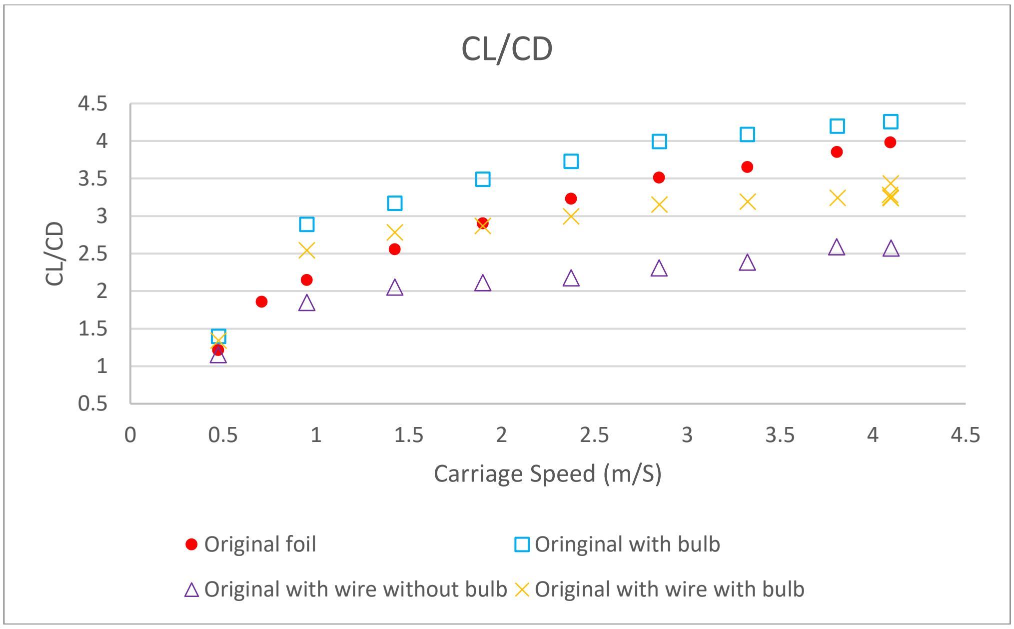

Figure 11. Lift drag ratio for foil with increased turbulence and horizontal in normal position with bulb

4 FULLY VENTILATED FLOW

4.1 Water sprayer methodology

The formation of a ventilated cavity was initially triggered for the unmodified foil using the water sprayer allowing the effects of ventilation to be observed. Water was sprayed at the leading edge of the strut where the strut intersected the free surface. This breaks the free surface seal around the strut while simultaneously causing the flow to separate resulting in two of the required conditions for ventilation to occur (Binns & Barden, 2012). The ventilated cavity was observed to travel down the strut from the free surface to the horizontal as shown in Fig. 12.

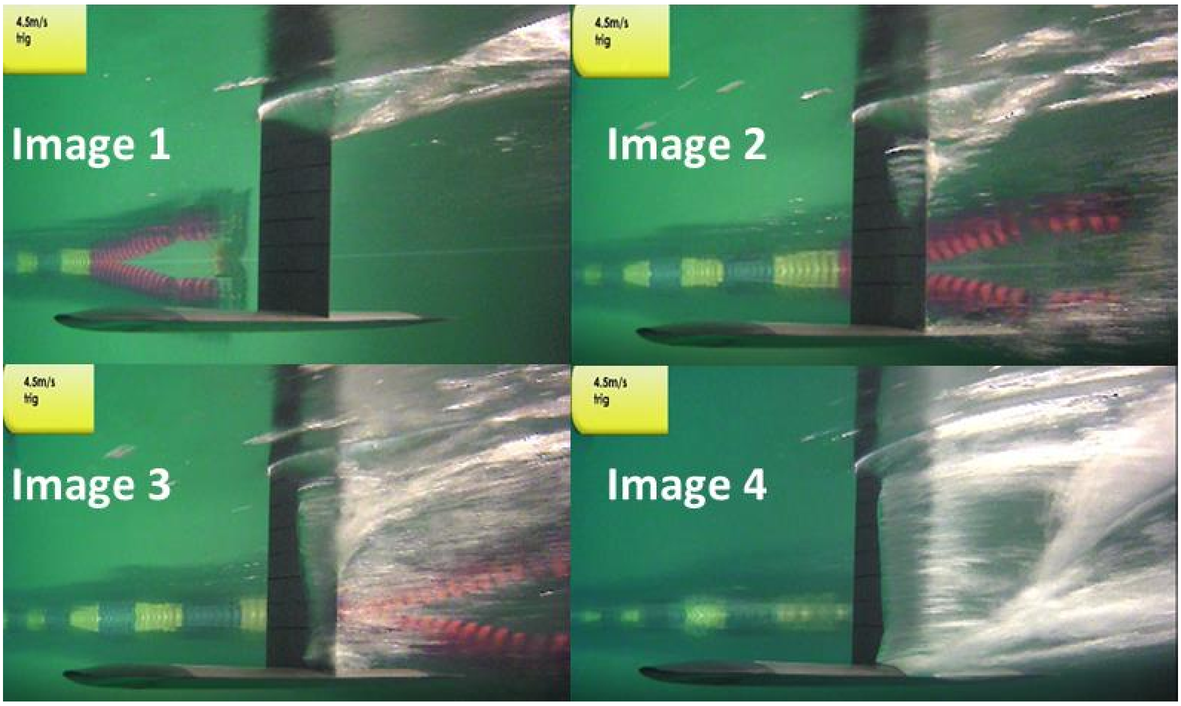

Figure 7. Development of ventilated cavity

4.2 Wire based triggering methodology

Formation of the ventilated cavity is dependent on the presence of flow separation (Binns & Barden, 2012) which occurs due to the presence of an adverse pressure gradient. The presence and position of a device to increase the flow turbulence, a wire in this experiment, results in the angle of attack at which flow separation occurs to vary (Chen & Chen, 2021). The turbulence generator results in the flow separating from the foil in conditions it otherwise wouldn't creating the conditions for a ventilated cavity to form.

The formation of a ventilated cavity without the use of the water sprayer is dependent on the position of the flow trip. No ventilation was observed with the wire positioned 10mm from the leading edge. Extensive stable ventilation was observed with the wire positioned 30mm and 40mm from the leading edge.

Moving the flow trip closer to the trailing edge, 50mm from leading edge, leads to cases of previously stable ventilation becoming unstable. Moving the flow trip towards the trailing edge increases the likelihood that it is within the adverse pressure gradient where it results in the laminar boundary layer separating before the flow then reattaches with no flow separation visible at the trailing edge (Roberts, et al., 2017). The initial flow separation followed by reattached explains the formation of the ventilated cavity followed by its rapid closure as shown below in Fig. 13.

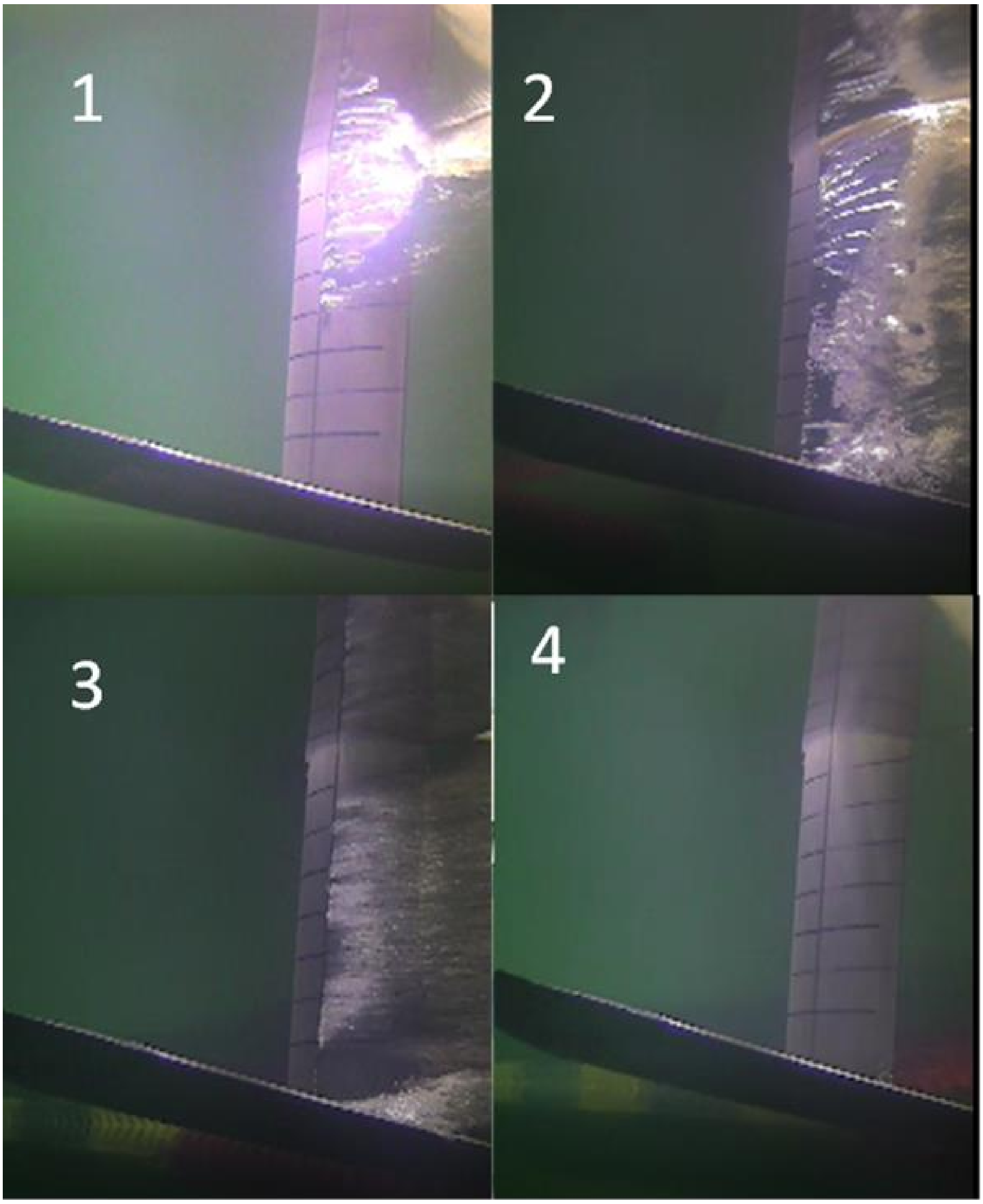

Figure 8. Formation and closure of the ventilated cavity due to turbulence generating wire

A tip vortex was observed to form when the strut was tested with the flow trip without the horizontal as shown below in Fig. 14. No vortex was observed when the foil was tested in any configuration without the flow trip fitted. The presence of the flow trip leads to an increase in the diameter of the vortex (McAlister & Takahashi, 1991) resulting in the vortex becoming visible in the images. The increased diameter of the vortex allows air to travel down hence ventilation occurring. The horizontal acts as an end plate which reduces the size of the vortex forming at the tip. The vortex forms due to roll up occurring due to the fluid travelling around the tip from the pressure to the suction side, the horizontal reduces this flow (Lee & Gim, 2013).

Figure 9. Tip vortex ventilation on strut at 138mm submergence, 4.5m/s and 6 degrees of yaw

4.3 Characteristics of the ventilated cavity

Several cases where visible ventilation occurred on the horizontal were observed as shown below in Fig. 15.

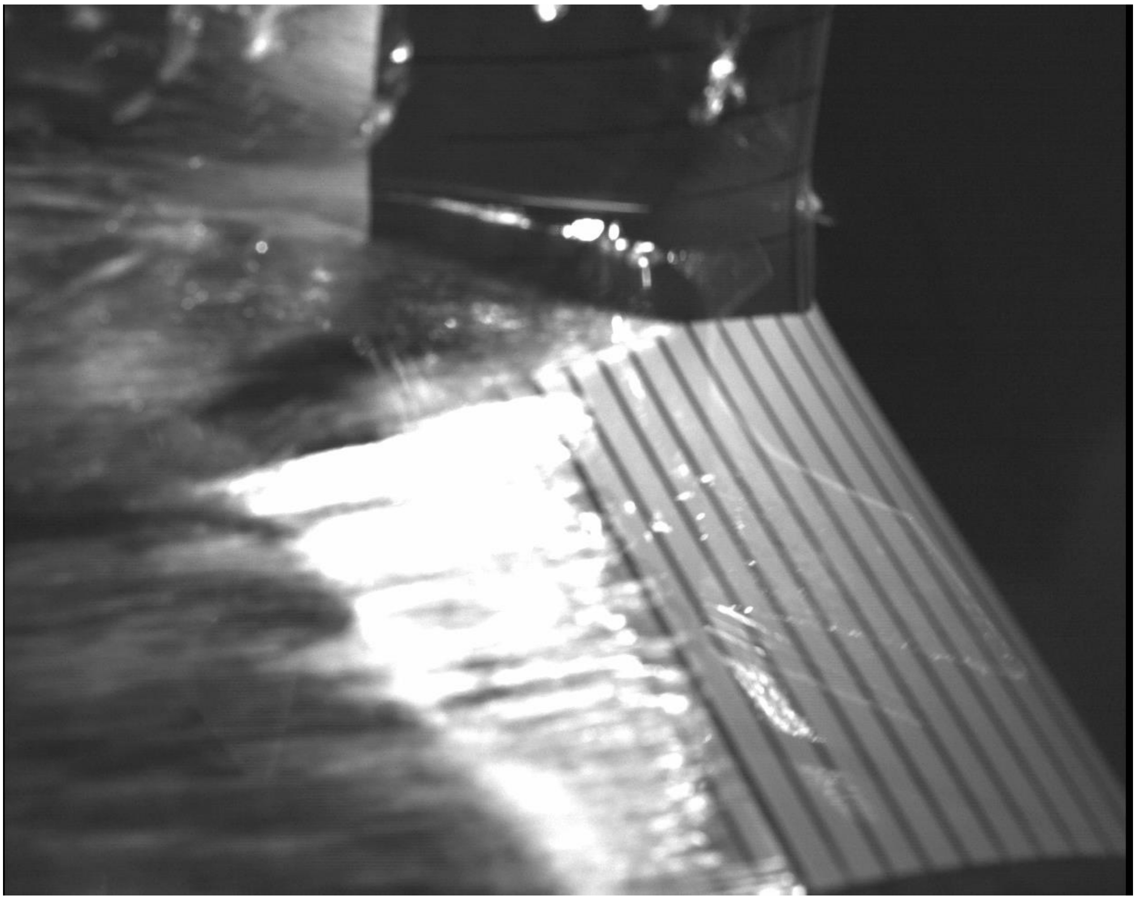

Figure 10. Visible ventilation of foil horizontal

Ventilation of the horizontal was observed for all yaw angles with it being significantly more likely to occur at higher test speeds. Additionally it was more likely to occur with the water spray in use and at lower submergence depths. No cases occurred when the bulb was fitted to the foil. Fourteen cases of horizontal ventilation were observed with twelve occurring when the wire and water sprayer were used together. The development of the visible ventilated cavity is shown below in Fig. 16.

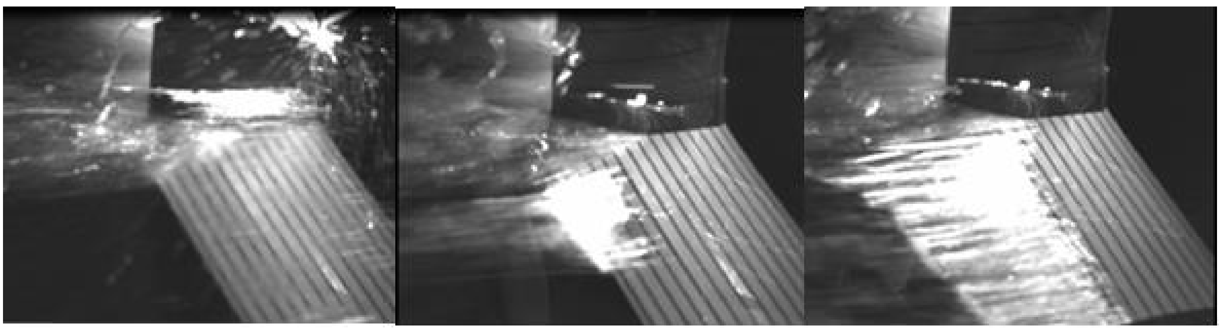

Figure 11. Development of ventilation on horizontal

Formation of a visible ventilated cavity around the horizontal occurred in a number of stages with ventilation first becoming visible around the strut. Unstable flashes of ventilation then become visible typically travelling outwards along the horizontal towards the strut tip. Eventually the ventilation travelling outwards became sufficiently stable to cover the whole foil horizontal. In many of the test cases observed unstable ventilation propagated outwards towards the horizontal tip multiple times before it became stable across the whole length of the horizontal. The pressure on the suction side of the horizontal is at a lower pressure than the ventilated cavity. This results in the expansion of the ventilated cavity in a spanwise direction into the low-pressure region which forms on the top surface of the horizontal. The behaviour of the flow around the junction is significant with the position and nature of the horseshoe vortex being an area worthy of further work.

The characteristics of the ventilated cavity shape are dependent on position of the wire when the water sprayer is used to induce ventilation. The wire being closer to the leading edge results in a visible vortex leaving the strut trip rising towards the free surface giving the cavity a triangular shape. The ventilated cavity becomes more even and clearer when the wire is positioned closer to the trailing edge. Fig. 17 below shows this comparison with the left image showing the wire at 30mm and the right image 10mm from the leading edge of the strut. Ventilation in this case had been induced by the water sprayer.

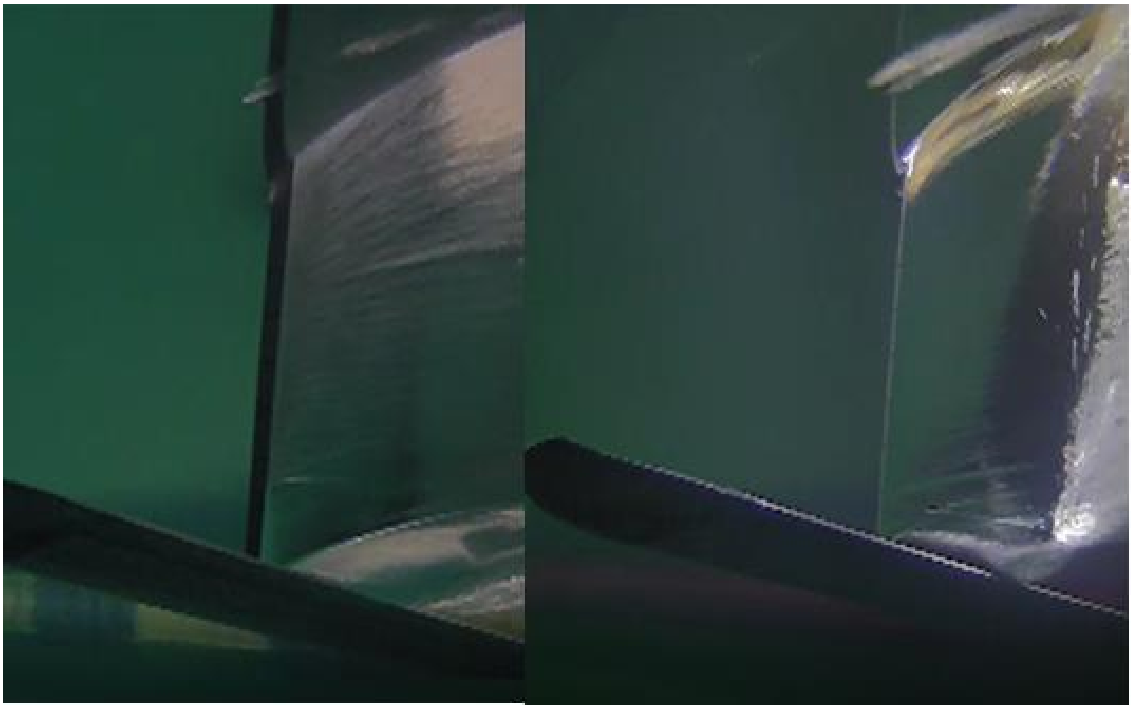

Figure 12. Ventilated cavity at 4.25m/s, 2 degrees, 213mm submergence

Fitting the bulb led to the removal of the horizontal from the visible ventilated cavity. The ventilation around the strut on the unmodified foil travels down the strut contacting the horizontal as shown in Fig. 18. It then begins to rise towards the free surface as the distance from the trailing edge of the strut increases. The size of the ventilated cavity reduces as distance from the strut increases. This results in the horizontal being underneath the visible ventilated cavity when the bulb is fitted as shown in Fig. 19 below.

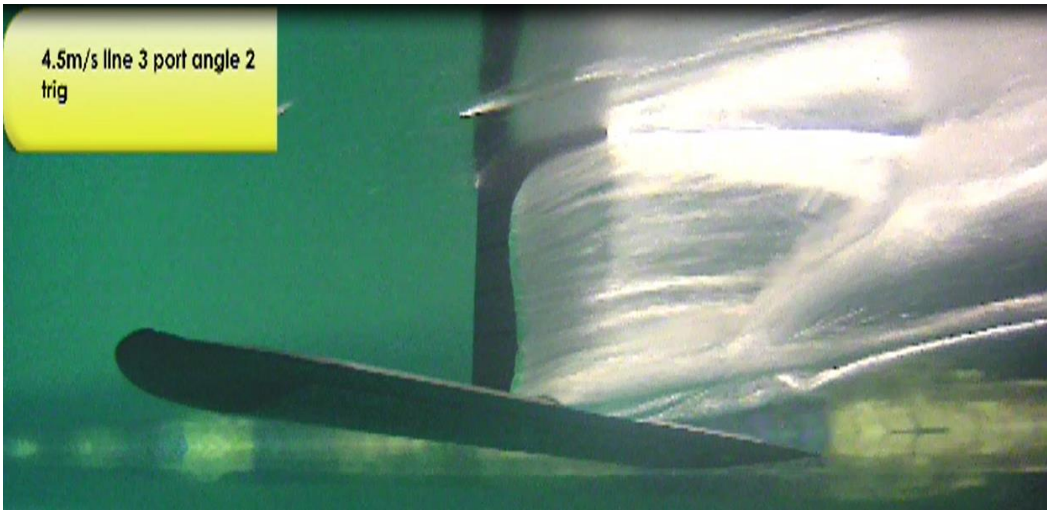

Figure 13. Ventilated cavity of unmodified foil

Figure 14. Ventilated cavity of foil fitted with bulb

5 CONCLUSION

A new technique capable of inducing repeatable ventilation of the foil at tank testing speeds has been found. Fitting a turbulence generating wire to the strut results in flow separation occurring allowing the formation of a ventilated cavity. Further work to explore alternative methods, e.g. sand the foil surface, capable of increase the turbulence would be of benefit. The importance of the positioning of this wire was shown with the wire position determining if ventilation occurred. This triggering method will be of practical benefit for future studies.

The performance of the foil with the horizontal in three positions was quantified with reduced submergence shown to decrease the performance of the foil in the majority of cases tested. Speed was identified as an important parameter with local maximums and minimums apparent at low speeds in the lift drag coefficients. This makes optimising the horizontal position, submergence depth and speed key to improving the foil performance.

Fitting of a bulb, to the junction between the strut and horizontal, was shown to reduce the drag coefficient of the foil. Further work to optimise the shape of the bulb would likely improve this further.

Moving the horizontal backwords leads to an improvement in the lift drag ratio with substantial reductions in the drag coefficient observed. This horizontal position also had substantial benefits when fully ventilated flow occurred as the horizontal was removed from the visible ventilated cavity.

The formation of a tip vortex leading to ventilation was observed when the strut was tested along with the wire fitted. Visible differences in the ventilated cavity were seen as the position of the wire was modified. The images appear to show an area of turbulence travelling backward and upwards away from the base of the strut when the wire is positioned closer to the trailing edge.

Visible ventilation was observed on the horizontal with it travelling outwards from the base of the strut. This was observed to be more likely to occur with the wire fitted close to the leading edge of the strut. Low depth of submergence and the use of the water sprayer were also key. Further analysis of the horseshoe vortex around the base of the strut is key to understand how the ventilation moves from the strut to the horizontal. This work would also help to inform the changes seen in the drag coefficient for the foil in fully wetted flow when it is fitted with the bulb.

Towing tank testing limits the speeds available making investigation of typical sailing speeds impossible. Use of CFD would provide the ability to investigate a larger range of cases.

6 Acknowledgements

The Kelvin Hydro Lab staff for building the test rig, modifying the foil and conducting the testing. Dr Saishuai Dai for supervising the project and advising on testing. Professor Day, Margot Cocard and others who developed the water sprayer triggering methodology. Arthur Trillio for collecting some of the data presented here. The research intern at Strathclyde program which funded the completion of this work.

7 References

Andersson, R. & Granli, S., 2018. *Free Surface Effects on Horizontal Hydrofoils,* s.l.: s.n.
Andresson, A. et al., 2018. Design of a Foiling Optimist. *Journal of Sailboat Technology.*
Beaver, B. & Zseleczky, J., 2009. *Full Scale Measurements on a Hydrofoil International Moth.* Annapolis, s.n.
Binns, J. & Barden, T., 2012. *On the Road to Establishing Ventilation Probability for Moth Sailing Dinghies.* Launceston, s.n.
Chen, H. & Chen, B., 2021. Aerodynamic Performance Enhancement of Tiltrotor Aircraft Wings Using Double-Row Vortex Generators. *International Journal of Aeronautical and Space Sciences,* pp. 802 - 812.
Day, S., Cocard , M. & Troll, M., 2019. *Experimental Measurement and Simplified Prediction of T-foil Performance for Monohull Dinghies.* Annapolis, s.n.
Duncan, J. H., 1983. The breaking and non-breaking wave resistance of a two-dimensional hydrofoil. *Journal of Fluid Mechanics,* Volume 126, pp. 507 - 520.
Korulla, M. & Sha, O. P., 2012. Artificially Ventilated Conventional Hydrofoils – An Experimental Investigation. *International Shipbuilding Progress,* Issue 59, pp. 129 - 162.
Lee, G.-W. & Gim, O.-S., 2013. Flow characteristics and tip vortex formation around a NACA 0018 foil with an endplate. *Ocean Engineering.*
McAlister, K. W. & Takahashi, R. K., 1991. *NACA 0015 Wing Pressure and Trailing Edge Vortex Measurements,* s.l.: NASA.
Roberts, L. S., Finnis , M. V. & Knowles, K., 2017. Forcing Boundary-Layer Transition on a Single-Element Wing in Ground Effect. *Journal of Fluid Engineering.*
Xing, T., Wheeler, M. P. & Matveev, K. I., 2019. Numerical study of high-lift hydrofoil near free surface at moderate Froude numbers. *Jounal of Hydrodynamics.*